Journal of the European Ceramic Society **6** (1990) 291–301

High Temperature Strength of Silicon Nitride HIP-ed with Low Amounts of Yttria or Yttria/Alumina

Anders Micski & Bill Bergman

Department of Physical Metallurgy and Ceramics, Royal Institute of Technology, 100 44 Stockholm, Sweden

(Received 20 April 1990; accepted 29 May 1990)

Abstract

Three HIP-ed silicon nitride materials were studied, two of which were produced from KemaNord powders and the third one produced from UBE silicon nitride powder. The materials were alloyed with 2·5 wt% Y_2O_3. Besides this one of the KemaNord materials also contained 1 wt% Al_2O_3. Fracture strength and fracture toughness were determined as a function of temperature (20–1500°C). The KemaNord materials' susceptibility to slow crack growth was studied by using two different cross-head speeds when fracture testing the specimens. An extensive fractography was made to determine the fracture initiating flaw. The differences in behaviour between the materials can be explained by differences in composition, impurity content and/or grain size.

Es wurden drei durch heißisostatisches Pressen hergestellte Siliziumnitridwerkstoffe verglichen. Zwei der Siliziumnitridausgangspulver stammten von Kema Nord und das Dritte wurde von UBE hergestellt. Den Ausgangspulvern wurden je 2·5 Gew.% Y_2O_3 zugegeben. Daneben enthielt eines der KemaNord Pulver außerdem 1 Gew.% Al_2O_3. Die Bruchfestigkeit und die Bruchzähigkeit wurden in Abhängigkeit von der Temperatur (20–1500°C) ermittelt. An den KemaNord Materialien wurde das langsame Rißwachstum während der Festigkeitstests mit Hilfe von zwei Querhauptgeschwindigkeiten untersucht. Um den bruchauslösenden Riß zu bestimmen, wurden ausgedehnte Untersuchungen der Bruchflächen durchgeführt. Das unterschiedliche Verhalten der einzelnen Materialien kann auf Unterschiede in der Zusammensetzung, den Anteil an Verunreinigungen und/oder die Korngröße zurückgeführt werden.

On a étudié trois types de nitrure de silicium pressé isostatiquement à chaud: deux étaient élaborés à partir de poudres KemaNord et un à partir de poudre UBE. On a allié ces poudres avec 2·5% massiques de Y_2O_3. Une des poudres KemaNord contenait également 1% massique de Al_2O_3. On a mesuré leur résistance à la rupture et leur ténacité en fonction de la température (20–1500°C). On a étudié la sensibilité des matériaux KemaNord à la propagation lente des fissures en utilisant deux vitesses différentes lors de l'essai de fissuration. Les défauts provoquant la rupture ont été révélés par des analyses fractographiques poussées. Les différences de comportement entre les matériaux peuvent être expliquées par leurs compositions, leur teneurs en impuretés et/ou la taille de leurs grains.

1 Introduction

Silicon nitride is currently being evaluated for use at elevated temperatures (≥ 1000°C), e.g. for use in gas turbines, because of its high strength and good thermal shock resistance. Since Si_3N_4 is a covalently bonded solid, the self diffusivity is low and this makes sintering difficult. Sintering aids are therefore required to provide the liquid phase necessary for densification. The sintering aid(s) react with the silica on the surface of the Si_3N_4 particles to produce the liquid phase, which, in most cases, results in a residual glass phase determining the high-temperature performance. By using oxide additives, e.g. yttria, a more refractory glass phase can be produced, which may be subjected to a heat treatment in order to crystallize and hence increase the high-temperature performance.[1] However, the

Journal of the European Ceramic Society 0955-2219/90/$3.50

amount of sintering aids has to be optimized in order to prevent the precipitation of phases which might be oxidation sensitive.[2] Hot isostatic pressing (HIP) offers a means of producing fully dense materials with low amounts of sintering aids, thus decreasing the amount of glass phase present in the final product. An additional advantage with the HIP technique is that intricately shaped parts of near-net shape can be produced.

This study was undertaken to characterize the flexural strength as a function of temperature (20 to 1500°C) for three HIP-ed materials with yttria or yttria/alumina as sintering aids. Fractography and EDS analysis were utilized to identify the fracture initiating flaw.

2 Experimental

Three series of Si_3N_4 samples were compared in the present study. Two series were produced from powder supplied by KemaNord Industrikemi (Ljungaverk, Sweden) (grade P95 J), one alloyed with 2·5 wt% Y_2O_3 (denoted KN0), the other alloyed with 2·5 wt% Y_2O_3 + 1 wt% Al_2O_3 (denoted KN1). A third series, produced from Si_3N_4 supplied by UBE Industries (Tokyo, Japan) (grade SNE-10), was alloyed with 2·5 wt% Y_2O_3 (denoted UBE0). Table 1 summarizes the results from chemical and phase analysis of the powders, together with the results from BET measurements of the specific surface area.

Prior to HIP, the mixture of silicon nitride powder and additives were ball milled for 48 h using Si_3N_4 balls and containers with petrol as milling medium. After evaporation of the liquid, the powder was cold isostatically pressed at 300 MPa. Hot isostatic pressing was done by ABB Cerama (Robertsfors, Sweden) at 1750°C, 200 MPa and with a holding time at maximum temperature of 1 h, using the ABB Cerama proprietary encapsulation method.[3] A heat treatment at 1400°C for 3 h was applied to produce a more refractory grain boundary phase.

Table 1. Characteristics of the silicon nitride powders

Element	*Powder*	
	UBE-SNE-10	*P95J*
Oxygen (wt%)	1·5	0·95
Iron (ppm)	50	400
Calcium (ppm)	<10	<100
Aluminium (ppm)	<10	600
Nitrogen (wt%)	38·2	—
Chlorine (ppm)	50	—
Free silicon (wt%)	—	0·2
Carbon (wt%)	—	0·5
Phase content, $\frac{\beta}{\alpha+\beta}$	0·03	0·09
BET surface area (m^2/g)	13	3·5–5

Bend bars with the dimensions 3·5 × 4·5 × 50 mm^3 were supplied by ABB Cerama in as-cut condition. The edges had been chamfered in order to avoid fracture initiation from edge flaws introduced during cutting. Some specimens were tested after polishing using 45 μm, 14 μm and 6 μm diamond slurries.

The flexural strength was evaluated in four-point bending (inner/outer span 19/38 mm respectively) in a universal testing machine at room temperature and from 1000 to 1500°C in an ATS split furnace. At elevated temperatures the specimens were held at the test temperature for 15 min to achieve thermal equilibrium, during which a preload corresponding to 20 MPa was applied. Two different cross-head speeds were used, 0·5 mm/min corresponding to a loading rate of 16 MPa/s, and 0·005 mm/min, corresponding to 0·16 MPa/s. Time to fracture was of the order of 30 s and 45 min,

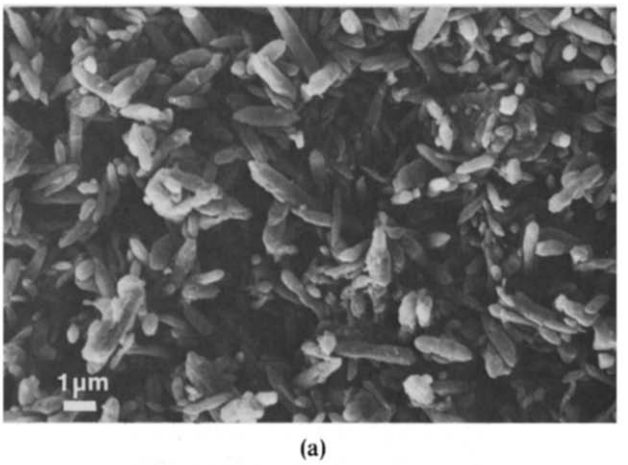

(a)

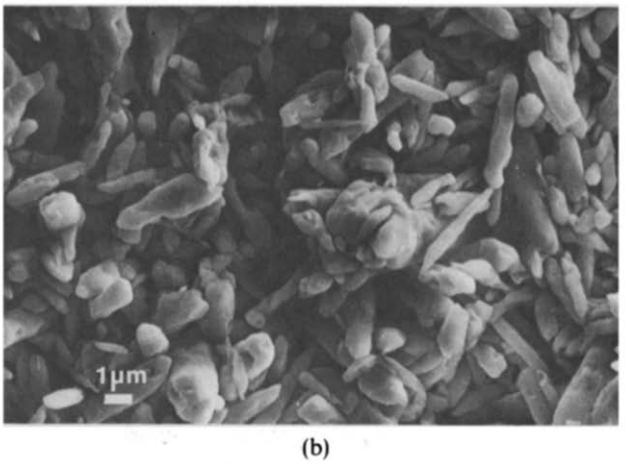

(b)

Fig. 1. The microstructure of HIP-ed Si_3N_4 made from (a) UBE powder and (b) KemaNord powder. The specimens have been etched in a molten mixture of KOH and NaOH.

respectively. The slow loading rate was only used on the KN materials at 1000 and 1200°C.

Fracture toughness was evaluated using the indentation-strength-in-bending (ISB) method.[4] In order to minimize the size and number of crack systems, a Knoop indent was made, carefully positioning the large diagonal perpendicular to the long side of the specimen, using a load of 50 N. The specimens were polished prior to indentation. The UBE0 specimens were additionally polished after indentation.[5] In order to prevent crack healing during the heating period a preload corresponding to 40 MPa was used, corresponding to a stress intensity factor of about 15% of the fracture toughness (K_c).

All fracture surfaces were studied in SEM (JEOL 840 equipped with a windowless EDS LINK detector). In order to characterize the microstructure the three materials were etched in a mixture of molten NaOH and KOH for 30 s. The mean grain diameter for UBE0 is about to 0·3 μm (see Fig. 1(a)), and about 0·9 μm for KN0 and KN1 (see Fig. 1(b)). The aspect ratio for all three materials is about 4.

3 Results

3.1 Chemical composition and phases

The oxide additives help in promoting a fully dense material. In particular the addition of Al_2O_3 has a wide range of effects, e.g. lowering the sintering temperature. The disadvantages include suppressing crystallization of intergranular phase, which in turn decreases the high temperature fracture strength, and promotes the development of slow crack growth (SCG) as discussed by Smith & Quackenbush.[6]

According to the phase diagram Si_3N_4–SiO_2–Y_2O_3–YN the material should be within the compatibility triangle defined by Si_3N_4–Si_2N_2O–$Y_2Si_2O_7$. Compositions within this triangle should not result in the type of intergranular crystalline phases susceptible to oxidation involving large volume changes thus degrading the materials strength, as discussed by Lange *et al.*[2] and Smith & Quackenbush.[7]

X-Ray diffraction analysis, using CuK_α-radiation, on the HIP-ed materials showed primarily β-Si_3N_4 and traces of Si_2N_2O. Furthermore, the KemaNord material without alumina contained traces of $Y_2Si_2O_7$. These analyses indicate that the sintering aids and the SiO_2 which always are present on the Si_3N_4 grains primarily form a residual glass phase situated in the grain boundaries of the β-Si_3N_4. The effect of the resulting residual glass phase on the high temperature strength of Si_3N_4 is highly dependent on the viscosity of the glass phase, which is a function of temperature and the amount of impurities in the material. A low viscosity of the grain boundary glass phase will enhance the probability of deformation processes, like grain boundary sliding, to occur, thus reducing the strength. It is also possible, however, that a viscous glass phase will blunt existing flaws and thereby increase the strength. The analysis of the powder (see Table 1) shows that the Si_3N_4 powder supplied by KemaNord contains a higher amount of iron and aluminium impurities than the UBE powder.

Table 2. Results from chemical analysis (wt%)

Material	*Al*	*Y*	*O*	Al_2O_3	Y_2O_3	SiO_2
KN0	—	1·98	2·24	—	2·51	3·2
KN1	0·58	2·03	2·59	1·10	2·58	2·87
UBE0 (estimated)	—	—	3·1	—	2·5	4·8

A chemical analysis was made on HIP-ed KemaNord material with respect to Al, O and Y (see Table 2). All Al and Y are assumed to be combined with oxygen as Al_2O_3 and Y_2O_3, respectively, and the remaining oxygen is assumed to be present as SiO_2. The figures in Table 2 give an indication of the amount of amorphous silica, and thus the amount of glass phase, present in the material. No chemical analysis was made on HIP-ed UBE material and the oxygen content was therefore estimated by assuming that the UBE powder picked up the same fraction of oxygen during milling as the KemaNord powder, not taking into account the larger specific surface area of the UBE powder, which would give a higher uptake of oxygen than the figures in Table 2 indicate.

3.2 Flexural strength versus temperature

The mean strength of the three materials in as-cut condition, based on 5–7 bend bars, is plotted as a function of temperature in Fig. 2. The strength of UBE0 is higher than for either KN0 or KN1 at temperatures $\geq$ 1000°C and was approximately the same at 1000 and 1200°C, after which it dropped. The KN0 and KN1 materials were also tested in the temperature range between 1000 and 1200°C and the results in Fig. 2 show that KN0 maintains its strength to about 1200°C after which it drops in about the same way as the strength for UBE0. (The strength data for KN0 after testing at 1100°C seems to be much too low, compared to the strength values at 1080 and 1150°C. The most probable explanation is that some error was present in the load calibration at 1100°C.) Two specimens of KN0 were tested at

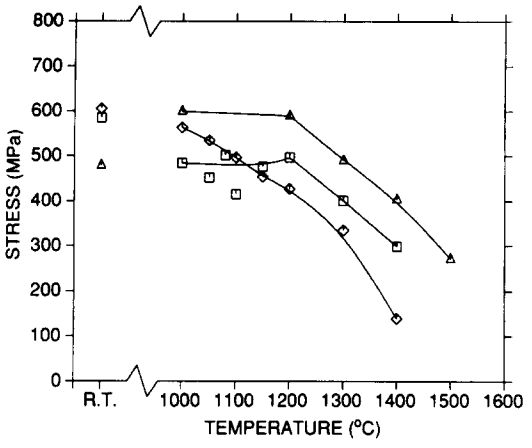

Fig. 2. Flexural strength as a function of temperature. △, UBE0; □, KN0; ◇, KN1, all as received.

1500°C but they could not sustain the preload of 20 MPa without considerable softening. The strength of the KN1 material dropped continuously from 1000 up to 1400°C. No testing was done at 1500°C.

A number of specimens were polished and subsequently tested at elevated temperatures (see Table 3) where the mean strengths for as-received and polished specimens are compared at the same temperature for each material. Six specimens were tested for each material and temperature, except for KN0 at 1000°C where 17 bend bars were fractured. The result from high-temperature fracture testing of UBE0 specimens has been reported previously[5] and neither at 1000°C nor at 1300°C was any significant difference in fracture strength obtained comparing as-received and polished specimens (see Table 3). The comparison was made using Student's *t*-test at a level of significance of 10%.[8] The same conclusion holds for KN0 at 1000°C, but at 1100°C, however, a significant difference was obtained, comparing as-received and polished specimens. However, since the strength testing at 1100°C of unpolished specimens was believed to have given too low values, it is more appropriate to compare the strength of the polished bendbars with the results of as-received KN0 specimens tested at 1080°C. In doing so, no significant strength difference was found. At 1200°C the mean strength for as-received specimens was higher than for polished specimens, but due to the large standard deviation the difference in mean strength was not found to be significant, using a significance level of 10%. The testing of the KN1 material gave no significant difference between as-received and polished specimens at any of the used temperatures. Thus, the conclusion is that the polishing did not have any effect on the mean strength at elevated temperatures for any of the three materials. The reason for this will be discussed later.

Table 3. Comparing fracture stresses of as-received and polished specimens

Material	*Temperature (°C)*	*Specimen strength (MPa)*	
		As-received[a]	*Polished*[a]
UBE0	1 000	599·5 (116·4)	605·2 (46·2)
UBE0	1 300	490·0 (43·6)	508·2 (81·9)
KN0	1 000	484·2 (46·2)	463·4 (69·9)
KN0	1 100	502·0[b] (44·2)	485·7 (49·2)
KN0	1 200	497·1 (101·8)	427·6 (34·4)
KN1	1 000	563·4 (86·2)	573·0 (76·2)
KN1	1 100	496·7 (56·9)	498·7 (52·5)

[a] The values in parentheses are equal to one standard deviation.
[b] Strength data from testing at 1 080°C.

Differences in cutting and chamfering conditions between the three materials were initially suggested to be responsible for some of the differences in high temperature strength. Therefore the room-temperature strength of five unpolished bendbars and of five unpolished bendbars after a 30-min heat treatment at 1000°C was determined for each material. The results are summarized in Fig. 3 together with the strength data from 1000°C. No correlation between room temperature strength and strength at 1000°C was found. After the heat treatment, the strength of the three materials increased to about the same strength level (see Fig. 3). Fractography showed that the fracture initiating flaws at room temperature were in more than 90% surface flaws, independent of whether the specimens were tested before or after heat treatment, which shows that surface flaws are still the most dangerous type of flaws, but the heat treatment made them less severe.

The load–deflection curves were linear during strength testing at room temperature and from 1000

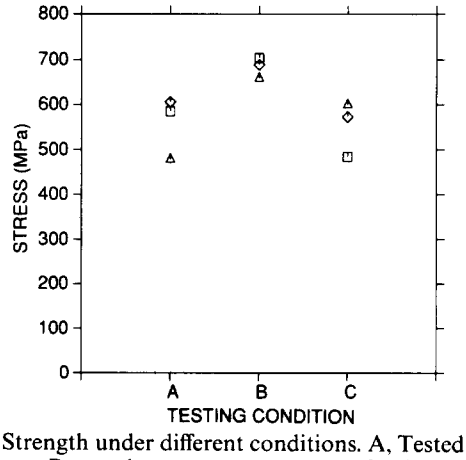

Fig. 3. Strength under different conditions. A, Tested at room temperature; B, tested at room temperature after heat treatment at 1000°C for 30 min; C, tested at 1000°C. △, UBE0; □, KN0; ◇, KN1.

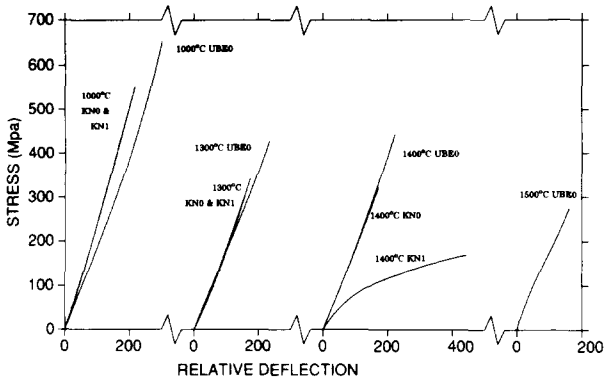

Fig. 4. Typical load–deflection curves.

up to 1300°C for the three materials. At 1400°C, however, KN1 showed a strong deviation from the ideal linear elastic behaviour (see Fig. 4). This deviation is attributed to the softening of the intergranular phase of KN1, which will be discussed in more detail later.

3.3 Fracture toughness

The fracture toughness was calculated using eqn (1), which has been used for semi-elliptical cracks, with a flaw depth (a) and a half-width (c) subjected to a bending moment with a maximum stress σ. The numerical correction factor M and the elliptical integral ϕ are functions of a/c. In this work M is assumed to be 1·03 corresponding to a/c equal to 0·8,[9] which is according to observations of fractured ISB specimens. An optical micrograph (Fig. 5) shows the fracture surface of a UBE specimen used for fracture toughness measurement at 1300°C. The indentation crack (light area), surrounded by the slow crack growth zone (see next paragraph) is apparent. Outside this zone the fast fracture area is seen. The flaw size a is measured at the depth where fast fracture begins.

$$K_c = \frac{M\sigma\sqrt{\pi a}}{\phi} \qquad (1)$$

K_c was measured at both room temperature and at high temperatures ($\geq$1000°C) for the three materials. UBE0 was tested up to 1500°C and KN0 was tested up to 1400°C. At temperatures above 1300°C the slow crack growth region for KN1 covered more than half the fracture surface and it was therefore not appropriate to determine the fracture toughness. The results are summarized in Fig. 6, in which can be seen that the fracture toughness at room temperature for the three materials is about the same $\approx 3{\cdot}6\,\mathrm{MPam}^{1/2}$. K_c was measured for UBE0 from 1200 up to 1500°C. At 1450°C is seen a maximum in K_c of $5{\cdot}2\,\mathrm{MPam}^{1/2}$ after which it drops to $3{\cdot}1\,\mathrm{MPam}^{1/2}$ at 1500°C. The

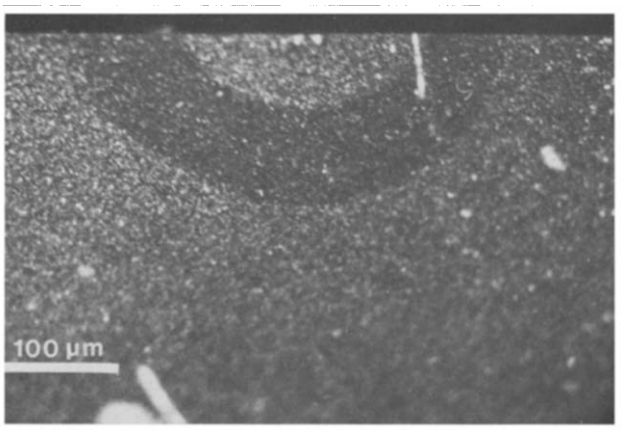

Fig. 5. Fracture surface of a Knoop-indented UBE specimen used for K_C measurement.

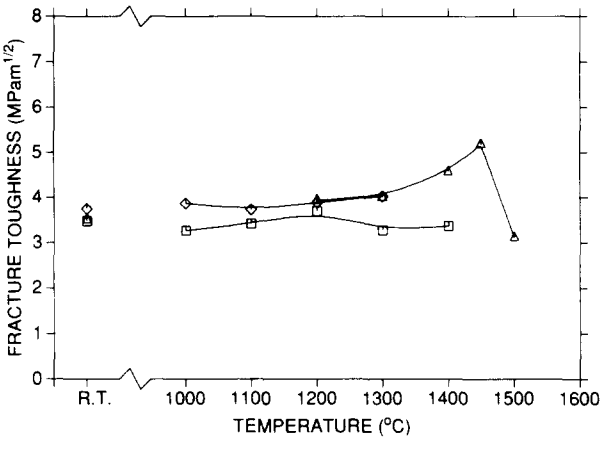

Fig. 6. Fracture toughness as a function of temperature. △, UBE0; □, KN0; ◇, KN1.

fracture toughness for both KN0 and KN1 was almost constant from 1000 to 1400°C for KN0 and from 1000 to 1300°C for KN1, the latter material having a slightly higher K_c of $3{\cdot}9\,\mathrm{MPam}^{1/2}$, compared to 3·3 for KN0.

3.4 Slow crack growth

A problem with many ceramics containing a glass phase is slow crack growth (SCG), i.e. the stable propagation of a crack at a stress intensity level below K_c. In order to measure the susceptibility for SCG, the mean strengths at 1000 and 1200°C were compared using two different crosshead speeds, 0·5 mm/min and 0·005 mm/min. This was only done for KN0 and KN1. Using eqn (2), where σ_1 and σ_2 are the mean strengths at a loading rate of $\dot{\sigma}_1$ and $\dot{\sigma}_2$, respectively, the n value can be calculated.[10] The results are summarized in Table 4, where the mean fracture strength value is based on 5–7 specimens for each crosshead speed.

$$(n+1)\log\left[\frac{\sigma_1}{\sigma_2}\right] = \log\left[\frac{\dot{\sigma}_1}{\dot{\sigma}_2}\right] \qquad (2)$$

Table 4. Results from n value determination

Temperature (°C)	Material	Mean fracture strength (MPa)[a]		n-value
		Crosshead speed		
		0·5 mm/min	0·005 mm/min	
1 000	KN0	484 (46)	447 (43)	57
1 000	KN1	563 (86)	486 (83)	30
1 200	KN0	497 (102)	401 (65)	20
1 200	KN1	427 (36)	357 (83)	25

[a] The values in parentheses are equal to one standard deviation.

Studies of fracture surfaces of Knoop-indented specimens revealed that slow crack growth appeared at temperatures >1200°C for the UBE material and at temperatures >1300°C for KN1. No indication of SCG was found in KN0.

3.5 Fractography

An extensive fractography was made in order to characterize the fracture initiating flaw, using both light optical microscopy (LOM) and SEM. HIP is considered as a superior means of producing dense materials. Nevertheless quite a few specimens failed due to volume flaws, e.g. inclusions, pores or processing defects like low-density regions caused by differential sintering because of the presence of agglomerates in the starting powder.

Let us start with discussing fractography of as-received specimens. As mentioned previously, more than 90% of the room-temperature testing resulted in failure initiated by surface defects. Based on the mean strength and the fracture toughness, and assuming half-circular surface cracks, an 'effective' crack depth was calculated to be 34 μm, 22 μm and 24 μm, for UBE0, KN0 and KN1, respectively. After a 30-min heat treatment at 1000°C, the 'effective' size of the defects decreased to 18 μm, 15 μm and 19 μm, respectively. When increasing the testing temperature to ≥ 1000°C, the amount of failures initiated from surface flaws in UBE0 decreased, but was still more than 60%. The amount of fractures initiated by volume defects was significantly higher in KN0 and depends strongly on the temperature; almost all specimens failed from volume flaws in the temperature range 1000–1150°C. When increasing the testing temperature to ≥ 1200°C, only 50% of the specimens failed from these defects. The amount of volume flaws in KN1 were 40%, independent of temperature range. No difference in the position of fracture-initiating flaw was found between testing with the slow and the fast cross-head speed. The slow cross-head speed however resulted in more well-defined fracture surfaces, making identification of the fracture-initiating flaw easier, which is an effect of a more stable crack propagation.

It is instructive to notice that merely testing the materials at room temperature will not make it possible to draw any reliable conclusions about what kind of defects control the high-temperature strength. Since it is of great importance to understand the nature of the defects which controls the high-temperature strength some typical volume defects will now be presented.

A common type of volume defect in the KN materials were inclusions containing silicon and iron together with nitrogen and oxygen, where the iron content varied from a few percent up to more than 50 at.%. These types of defects, found in both UBE0 and the KN materials, were more common in the latter ones. It is interesting to notice that between 1000 and 1150°C, 45% of the KN0 specimens failed from iron inclusions, but only 13% failed at 1200°C and above. This is in contrast to KN1, where the amount was about 25%, independent of temperature. A representative micrograph of a specimen failing due to this type of defect is seen in Fig. 7 showing a KN0 specimen tested at 1000°C. A high porosity area where the surrounding region contained iron can be seen. A similar type of defect is seen in Fig. 8, also in a KN0 specimen but tested at 1100°C. The surrounding region, rich in iron, shows melting to be beginning. Figure 9 shows a pore, found in a KN1 specimen tested at 1300°C, where the surrounding volume contains iron. This region seems to be completely melted and above the pore there is a small pit, which indicates the evolution of gases. Because of the high testing temperature the whole fracture surface has a glassy appearance due to the rapid oxidation of the exposed fracture surface. Impurities of titanium were found to cause

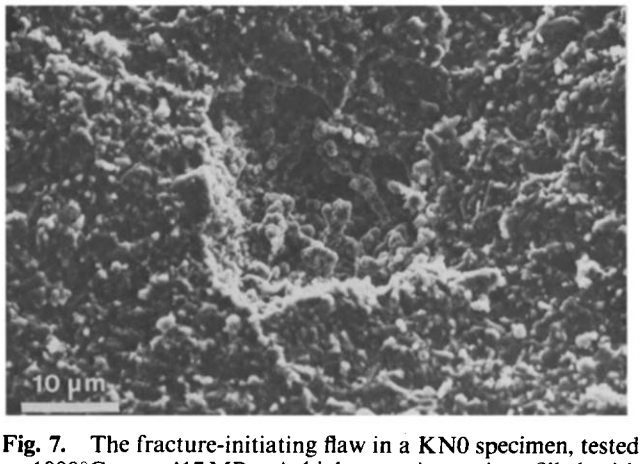

Fig. 7. The fracture-initiating flaw in a KN0 specimen, tested at 1000°C; $\sigma_f = 417$ MPa. A high porosity region, filled with material with a high iron content is seen.

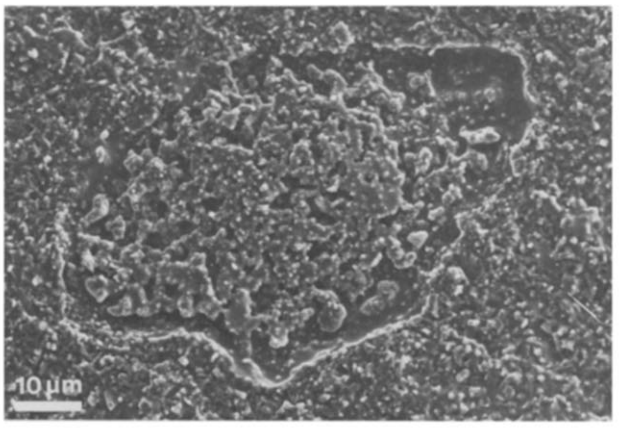

Fig. 8. The fracture-initiating flaw in a KN0 specimen, tested at 1100°C; $\sigma_f = 480$ MPa. The region was melted during strength testing and contains high amounts of iron.

failure in some of the UBE0 specimens at elevated temperature, which has been reported previously.[5]

In Fig. 10 is seen a fracture-initiating defect found in a KN1 specimen tested at 1200°C. The shape of the defect indicates that something, e.g. a textile fibre or a hair, has been lying here but no remnants of it were found during the fractography and EDS analysis. Figure 11 shows the fracture-initiating flaw in a KN0 specimen tested at 1200°C. A pore in which a crystal of yttria silicate has grown is seen, indicating that at some time the pore has been filled with a melt from which the crystal has precipitated.

A few defects caused by differential sintering, probably because of the presence of agglomerates in the powder, were found in the KN materials. In Fig. 12 an example of this type of defect, found in a KN0 specimen tested at 1000°C, is seen. Between the defect and the matrix an interfacial crack is found.

Due to the softening of the intergranular phase, the fracture surfaces will lose their characteristic fracture ridges and instead become smooth. This behaviour occurs above a temperature, specific for each material, which was between 1400 and 1500°C for UBE0 and between 1200 and 1300°C for the KN materials. All the fractured specimens behaved in the same manner, independent of fracture origin.

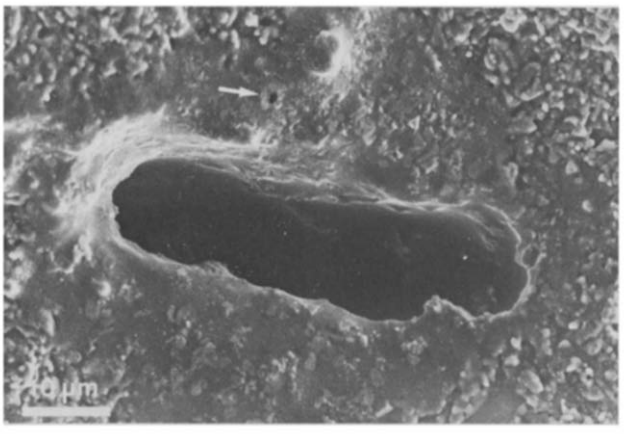

Fig. 9. The fracture-initiating flaw in a KN1 specimen, tested at 1300°C; $\sigma_f = 341$ MPa. The material immediately around the pore contains high amounts of iron. The arrow shows a pit, probably formed as a consequence of nitrogen evolution due to a reaction between Si_3N_4 and iron.

Fig. 10. The fracture-initiating flaw in a KN1 specimen, tested at 1200°C; $\sigma_f = 419$ MPa. The shape of the defect indicates that a textile fibre or a hair has been lying here.

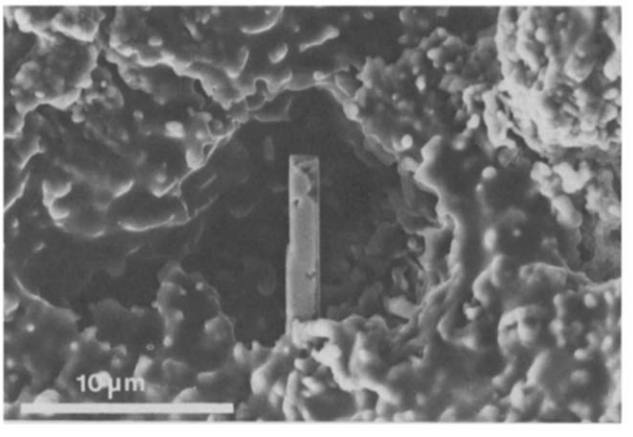

Fig. 11. A pore containing a crystal of yttrium silicate, the fracture-initiating flaw in a KN0 specimen, tested at 1200°C; $\sigma_f = 335$ MPa.

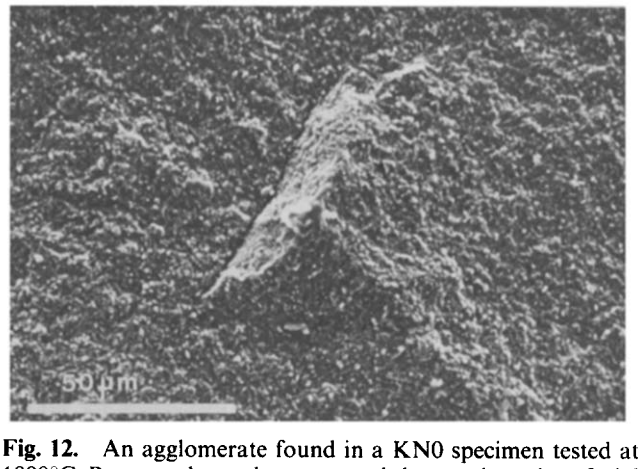

Fig. 12. An agglomerate found in a KN0 specimen tested at 1000°C. Between the agglomerate and the matrix an interfacial crack is found (see arrow); $\sigma_f = 496$ MPa.

Furthermore, at these high temperatures the fracture surfaces are rapidly oxidized and thus covered with a layer of amorphous silica, making it difficult to identify the fracture-initiating flaw.

At 1400°C, the fracture surfaces of KN1 are divided into two regions (Fig. 13(a)). The tensile side is at the top of the micrograph, along which a crack has initiated. Due to the viscous intergranular phase at this temperature, conditions have favoured the development of slow crack growth, during which the crack has propagated mainly in the intergranular phase, causing the rough appearance seen in the upper right of the figure. Because of the high testing temperature, a layer of glass is formed on the fracture surface, making fractography difficult, but if this glass phase is etched away, it can be seen that the crack propagates mainly intergranularly (Fig. 13(b)). This micrograph is a blow up of the SCG region in Fig. 13(a) after etching. The crack grows stably to a critical size, followed by fast fracture (see Fig. 13(c)) where it propagated mainly transgranularly. The micrograph is an enlargement of the fast-fracture region of the specimen in Fig. 13(a). Due to a higher value for the stress concentration factor along the sides of the specimen, the crack grows faster here and the border between the two regimes becomes curves.

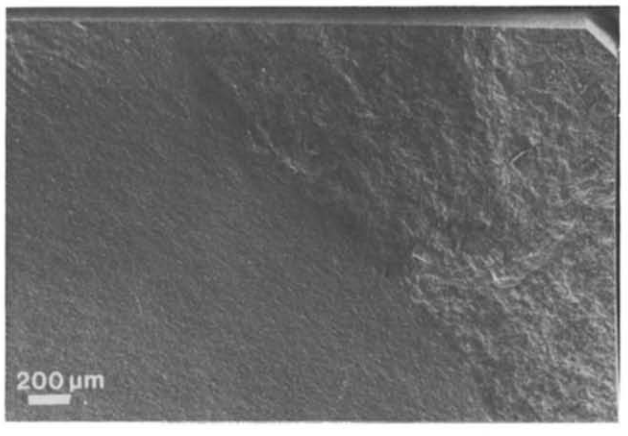

(a)

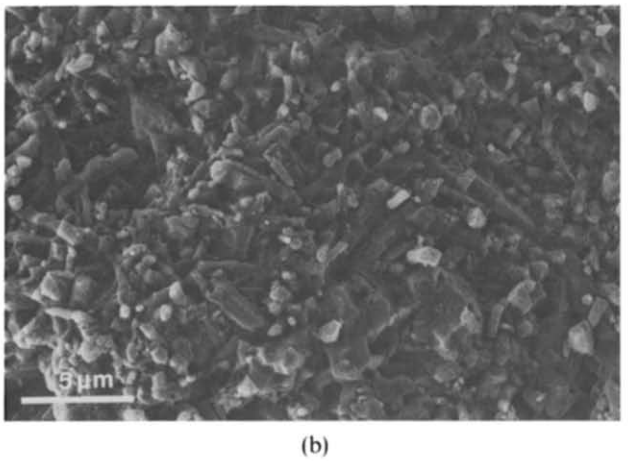

(b)

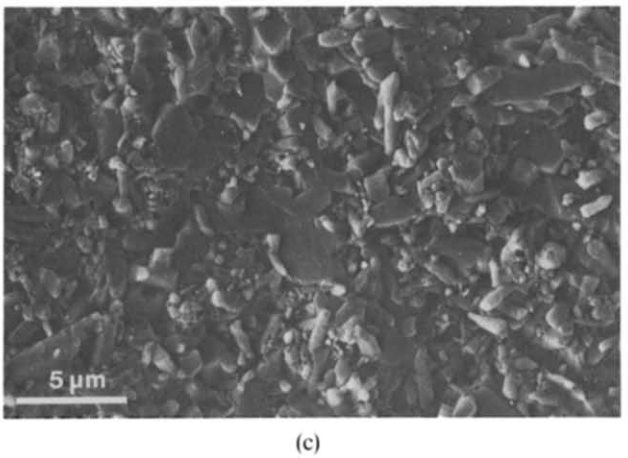

(c)

Fig. 13. (a) This micrograph shows the appearance of the fracture surface of a KN1 specimen, tested at 1400°C; the SCG region is seen in the upper right section. The specimen has been etched in a molten mixture of KOH and NaOH; (b) a magnification of the SCG region, showing that the crack has grown mainly intergranularly; (c) a magnification of the fast-fracture region. The proportion of transgranular fracture is much larger than in the SCG region.

4 Discussion

As shown in Fig. 2, UBE0 has a higher strength than the KN materials at temperatures above 1000°C. Furthermore it was shown that crack blunting occurs in these materials, since the room-temperature strength is increased after a heat treatment at 1000°C for 30 min for the three materials. This conclusion is further supported by the fact that the high-temperature fracture strength for as-received specimens is the same as for polished specimens. This is understood by considering that a flaw's severity is not only dependent on the size of the flaw but also on the radius of curvature at the crack tip. If the radius is large, i.e. if crack blunting has occurred, a reduction of flaw size (after e.g. polishing) will not result in any large increase in fracture strength. Thus, it is believed that blunting mechanisms, active during the heating and the time spent at the test temperature in order to achieve thermal equilibrium, will increase the radius of curvature of the crack tip of the flaws present. Two different blunting mechanisms have been considered; (1) oxidation of the crack tip, resulting in the formation of a surface layer of amorphous SiO_2, and (2) the viscous flow of the grain boundary glass phase, for which the driving force is the minimizing of surface energy. Both mechanisms will lead to an increased radius of curvature at the crack tip, thus resulting in a less severe flaw. Studies of fractured specimens shows that a thin layer of glass is formed

on the outer surfaces of the specimens at temperatures as low as 1000°C, indicating that oxidation is active at these temperatures. KN1 having a higher fracture strength compared to KN0 at 1000°C could be explained by assuming a higher oxidation rate of KN1, leading to a thicker oxide layer which blunts existing cracks more efficiently. The strength difference could also be the result of a more viscous grain boundary phase in KN1, due to the alumina addition, this making viscous flow at the crack tip an efficient mechanism for blunting. The result from the *n*-value determination is consistent with the latter explanation as the *n* value was lower for KN1 (≈ 30) compared to KN0 (≈ 60), this being a result of a more refractory grain boundary phase for KN0.

The difference in alumina content may also explain the difference in strength between the two KN materials at temperatures above 1000°C. Increasing the temperature further decreases the viscosity of the glass phase for KN1, resulting in a loss in fracture strength. The change in glass-phase viscosity with temperature does not seem to be as large for either UBE0 or KN0, since the high-temperature strength is constant from 1000 up to 1200°C. The *n* value for KN0 at 1000°C was found to be about 60, compared to around 30 for KN1 at the same temperature. At 1200°C the *n* value was around 22 for both materials. These values give an indication of the materials' susceptibility to slow crack growth and therefore an estimation of the relative viscosity of the glass phase. The *n* value of 60 at 1000°C for KN0 indicates that the viscosity of the glass phase is high, compared to KN1. When the temperature is raised to 1200°C, the glass phase softens, and due to the longer testing time, a crack can propagate in a way requiring lower energy, thus decreasing the *n* value. Consequently, the fast-fracture strength for KN0 drops when testing at temperatures higher than 1200°C. KN1 has a low *n* value at 1000°C, which indicates that the glass phase is already relatively viscous at this temperature, thus there is a continuous drop in strength for KN1 when the temperature is increased. At 1400°C the viscosity is low enough to enable a substantial slow crack growth during the testing time (see Fig. 13), further emphasized by the deflection curve (see Fig. 4) and by the fact that it was not possible to measure the fracture toughness value due to the 'softening' of the bend bar. No *n* value determination was made on UBE0, but there is an increase in fracture toughness value when increasing the temperature from 1200°C. This is due to blunting of the indented crack, a consequence of a softening glass phase, which also explains the reduction of strength and the development of slow crack growth at these temperatures. SCG in an UBE ISB specimen tested at 1300°C is seen in Fig. 5. Here the half-circular light region at the edge is the indented crack and the dark region surrounding this is the SCG region, outside which the fast-fracture region is seen. The smaller grain size of UBE0, favouring intercrystalline fracture, is probably the reason why SCG appears at lower temperatures (1300°C) than for KN1 (1400°C). No signs of SCG were found in KN0, due to the larger grain size compared to UBE0 and lower amount of sintering aid compared to KN1.

A possible explanation for the high-temperature strength for UBE0 being higher than the KN materials could be differences in the surface flaw populations. The room-temperature strength data, however, showed a significantly higher strength for the KN materials, and since the K_c values for the three materials are about the same, the surface flaws in UBE0 must be larger. Hence, the superior high-temperature strength for UBE0 is due to differences in microstructure, the amount of impurities present in the HIP-ed material and/or amount and viscosity of the intergranular glass phase.

The effect of grain size on fracture strength is not fully understood but it is commonly assumed that the grain size will limit the size of cracks at the surface or surrounding a pore. A material with a smaller grain size will therefore have smaller flaws, resulting in a higher fracture strength than a material with larger grains. The UBE material had a mean grain size of 0·3 μm compared with the KN materials which have a mean grain size of 0·9 μm. The aspect ratio was ≈ 4 for all three materials. Since the fracture toughness at room temperature was the same (3·5 $MPam^{1/2}$), and since fractures were almost exclusively initiated from surface flaws at this temperature, the as-cut UBE specimens probably were machined in such way that the surface damage was more severe than when machining the KN specimens, resulting in larger surface flaws despite the smaller grain size.

The grain size also has an effect on the distribution of the glass phase in the material. A large grain boundary area, i.e. small grains, distributes the same amount of intergranular phase on a larger area, resulting in a thinner grain boundary film and in smaller glass pockets in triple grain junctions. This will suppress deformation mechanisms like grain boundary sliding or cavity nucleation and thus increase the strength at elevated temperatures. UBE0 has a mean grain size which is a third of the grain size of the KN materials, giving a three times larger grain boundary area per volume unit. X-Ray

diffraction of HIP-ed material showed that the sintering aids mainly go into the intergranular glass phase, and subsequently the UBE material contains roughly 33% more glass phase compared to the KN materials (see Table 2). This difference in glass-phase volume is not large enough to make up for the difference in grain boundary area. Besides this, the low content of cations such as iron and aluminium in the UBE material (see Table 1) results in a high viscosity of the glass phase and thus a higher high-temperature strength.

Fractography revealed that a number of fractures were caused by inclusions containing silicon, iron, oxygen and nitrogen (see Figs 7–9). EDS analysis showed that the iron content varied from a few percent to more than 50 at.%. Furthermore, it was found that the nitrogen content decreased close to these inclusions, in many cases to zero, while the oxygen content was higher than in surrounding areas, up to 50 at.% in some cases. Different reaction formulae may be used to explain the effect of iron during HIP-ing, e.g. the direct decomposition of Si_3N_4 to silicon liquid and nitrogen may be enhanced by the presence of iron, which will decrease the activity of silicon:[11]

$$Si_3N_4 \rightarrow 3Si(l) + 2N_2(g) \quad (3)$$

A direct reaction between liquid iron and Si_3N_4 may also occur.[12]

$$3Fe(l) + Si_3N_4 \rightarrow 3FeSi + 2N_2(g) \quad (4)$$

or

$$6Fe(l) + Si_3N_4 \rightarrow 3Fe_2Si + 2N_2(g) \quad (5)$$

Furthermore it has been found that FeSi and Fe_2Si may precipitate from an iron-rich glass phase during cooling from the sintering temperature (Ekström, T., Sandvik Hard Materials, 1989, pers. commun.). At the HIP temperature, the areas containing iron will be melted, and the nitrogen gas, a product from the reaction between iron and silicon nitride, can result in a pore. During cooling from the HIP temperature, iron silicides precipitate and a defect with the appearance as in Fig. 7 is formed, where iron silicides have been precipitated from an iron-rich glass phase, of which residues still can be seen in the micrograph. The specimen is a KN0 specimen, fractured at 1000°C. When increasing the testing temperature to 1100°C the silicides begin to partially melt (Fig. 8) and at 1300°C the area surrounding the inclusion is completely melted (Fig. 9). According to the phase diagram Fe–Si, a eutecticum is found at 1207°C and dissolved nitrogen and impurities in the material should lower this temperature. It is also seen that the viscosity of the melt is low enough to enable nitrogen gas, which is a result from the reaction between iron and the silicon nitride, to be released and to form pits in the fracture surface. Due to the faster cooling rate of the split furnace, compared to the HIP, the silicides do not have any time to reprecipitate during the cooling after fracture.

Due to the relatively few specimens tested at each temperature, no definite conclusions can be made regarding the relation between strength and fracture-initiating flaw, but by studying the two specimens with the lowest strength for each material and temperature, and determining the fracture-initiating flaw for these, some trends for the KN materials could be established. Due to the few UBE specimens failing from volume defects and the difficulty in determining the type of volume flaw, it was not possible to do the same for this material. For KN0, however, 50% of the weakest specimens in the temperature range 1000 to 1150°C failed from iron inclusions. Increasing the temperature to 1200°C and above did not result in any failures from iron inclusions. In KN1, less than 20% of the weakest specimens failed from iron inclusions, independent of temperature. The KN0 material's sensibility to iron inclusions in the temperature range 1000 to 1150°C is most probably a consequence of the pores present due to the nitrogen evolution, which results from a reaction between iron and silicon nitride during HIP-ing. Above 1150°C the iron silicides melt and blunt the pores, thus decreasing the severity of the latter. (According to the phase diagram Fe–Si,[13] there is a low-melting eutectic at 1207°C. Dissolution of nitrogen and the presence of impurities will further decrease the liquidus temperature.) Generally it seems as if KN1 was less sensitive to iron inclusions than to KN0. This can be a result of (1) a lower viscosity of the glass phase, which makes it easier for impurities such as iron to become evenly distributed during HIP-ing, or (2) simply a consequence of the lower glass-phase viscosity, which promotes blunting of the nitrogen pores at temperatures as low as at 1000°C. Since iron inclusions were still present in the material, the latter explanation is more probable.

5 Conclusion

The flexural strength for three silicon nitride materials were characterized as a function of temperature (20 to 1500°C). Two materials were produced from Si_3N_4 powder supplied by

KemaNord Industrikemi and one from UBE Industries Y_2O_3 powder. All the materials contained 2·5 wt% yttria. Furthermore, one of the KemaNord materials was alloyed with 1 wt% alumina. The room-temperature strength was higher for the KN materials, due to less severe surface flaws. At elevated temperature ($\geq$ 1000°C), however, the UBE material exhibited a significantly higher strength than either of the KN materials. This is due to the higher purity of the silicon nitride powder and the finer particle size of the UBE powder. The strength was constant between 1000 and 1200°C, after which it decreased. At 1000 and 1050°C the Al_2O_3-containing KN material showed a higher fracture strength compared to the KN material sintered with Y_2O_3 only. This is because of a more efficient crack-blunting mechanism for the alumina-containing material, which is a consequence of a more viscous intergranular phase, which results in a viscous flow. The driving force for the viscous flow is the minimization of surface energy. With increasing testing temperature, the strength decreases continuously for this material, consistent with a decrease of the viscosity of the intergranular phase. The KN material HIP-ed with only Y_2O_3 as sintering aid retained its high-temperature strength up to 1200°C, after which the latter decreased.

An extensive fractography was utilized to identify the fracture-initiating flaw. The most common type at room temperature were surface flaws. With increasing temperature, volume defects become more severe. In KN0, volume flaws, especially iron inclusions, were the strength-controlling defects in the temperature range 1000 to 1150°C. At temperatures above 1150°C, the iron silicides soften and blunt the pores surrounding the inclusions and thus make them less severe. In KN1 the low viscosity of the glass phase can make the pore surrounding the iron silicides to blunt at temperatures as low as 1000°C. The UBE0 material was less sensitive to volume defects, and at elevated temperatures more than 60% of the failures were still caused by surface defects.

Acknowledgement

The financial support from the Swedish Board of Technical Development (STU) is acknowledged.

References

1. Gazza, G. E., Hot-pressed Si_3N_4. *J. Am. Ceram. Soc.*, **56** (1974) 662.
2. Lange, F. F., Singhal, S. C. & Kuznicki, R. C., Phase relations and stability studies in the Si_3N_4–SiO_2–Y_2O_3 pseudoternary system. *J. Am. Ceram. Soc.*, **60** (1977) 249–52.
3. Larker, H. T., Dense ceramic parts hot-pressed to shape by HIP. In *Emergent Process Methods for High Technology Ceramics*; ed. R. F. Davies, H. Palmow III & R. L. Porter. *Mater. Sci. Res.*, **17** (1984) 571–82.
4. Petrovic, J. J., Jacobson, L. A., Talty, P. K. & Vasudevan, A. K., Controlled surface flaws in hot-pressed Si_3N_4. *J. Am. Ceram. Soc.*, **58** (1975) 113–6.
5. Micski, A. & Bergman, B., High-temperature fracture of hot isostatically pressed Si_3N_4. In *Engineering with Ceramics 2, British Ceramic Proceedings*, ed. R. Freer, S. Newsam & G. Syers. Institute of Ceramics, Stoke-on-Trent, UK, 1987, pp. 45–54.
6. Smith, J. T. & Quackenbush, C. L., Phase effects in Si_3N_4 containing Y_2O_3 or $CeO_2$2. I. Strength. *Am. Ceram. Soc. Bull.*, **59** (1980) 529–32.
7. Smith, J. T. & Quackenbush, C. L., Phase effects in Si_3N_4 containing Y_2O_3 or CeO_2. II. Oxidation. *Am. Ceram. Soc. Bull.*, **59** (1980) 533–37.
8. Montgomery, D. C., *Design and Analysis of Experiments*. John Wiley & Sons, New York, 1984.
9. Petrovic, J. J., Effect of indenter geometry on controlled-surface-flaw fracture toughness. *J. Am. Ceram. Soc.*, **66** (1983) 277–83.
10. Khandelwal, P. K., Chang, J. & Heitman, P. W., Slow crack growth in sintered silicon nitride. In *Fracture Mechanics in Ceramics 8*, ed. R. C. Bradt, A. G. Evans, D. P. H. Hasselman & F. F. Lange. Plenum Press, New York, pp. 351–62.
11. Pasto, A. E., Causes and effects of Fe-bearing inclusions in sintered Si_3N_4. *J. Am. Ceram. Soc.*, **67** (1984) C178–C180.
12. Hermansson, L., Adlerborn, J. & Burström, M., Strength-controlling defects in HIP-ped silicon nitride. *Revue de Chimie Minerale*, **22** (1985) 467–72.
13. Kubaschewski, O., *Iron—Binary Phase Diagrams*. Springer-Verlag, Berlin and Verlag Stahleisen mbH, Düsseldorf, 1982, pp. 136–39.